Comparing quasiparticle GW + DMFT and LDA + DMFT for the test bed material $SrVO_3$

C. Taranto,[1] M. Kaltak,[2] N. Parragh,[3] G. Sangiovanni,[3] G. Kresse,[2] A. Toschi,[1] and K. Held[1]

[1]*Institute for Solid State Physics, Vienna University of Technology, 1040 Vienna, Austria*

[2]*University of Vienna, Faculty of Physics and Center for Computational Materials Science, Sensengasse 8/12, A-1090 Vienna, Austria*

[3]*Institut für Theoretische Physik und Astrophysik, Universität Würzburg, Am Hubland, D-97074 Würzburg, Germany*

(Received 6 November 2012; revised manuscript received 13 May 2013; published 11 October 2013)

We have implemented the quasiparticle GW + dynamical mean field theory (DMFT) approach in the Vienna *ab initio* simulation package. To this end, a quasiparticle Hermitization of the G_0W_0 self-energy a lá Kotani-Schilfgaarde is employed, and the interaction values are obtained from the locally unscreened random phase approximation (RPA) using a projection onto Wannier orbitals. We compare quasiparticle GW + DMFT and local density approximation (LDA) + DMFT against each other and against experiment for $SrVO_3$. We observe a partial compensation of stronger electronic correlations due to the reduced GW bandwidth and weaker correlations due to a larger screening of the RPA interaction, so that the obtained spectra are quite similar and agree well with experiment. Noteworthy, the quasiparticle GW + DMFT better reproduces the position of the lower Hubbard side band.

DOI: 10.1103/PhysRevB.88.165119 PACS number(s): 71.27.+a, 71.10.Fd

I. INTRODUCTION

The local density approximation (LDA) plus dynamical mean field theory (DMFT) approach[1–5] has been a significant step forward for calculating materials with strong electronic correlations. This is, because—on top of the LDA—DMFT[6,7] includes a major part of the electronic correlations: the local ones. In recent years, LDA + DMFT has been applied successfully to many materials and correlated electron phenomena, ranging from transition metals and their oxides to rare earth and their alloys, for reviews see Refs. 4 and 5.

For truly parameter-free *ab initio* calculations, however, two severe shortcomings persist: (i) The screened Coulomb interaction is usually considered to be an adjustable parameter in LDA + DMFT and (ii) the so-called double counting problem, i.e., it is difficult to determine the electronic correlations already accounted for at the local density approximation (LDA) level. These shortcomings are intimately connected with the fact that the nonlinear nature of density functional theory does not match with the many-body, Feynman-diagram structure of DMFT. Hence, it is not clear how to subtract correlation effects already included on the LDA level or how to express these as a self-energy to avoid a double counting with DMFT correlations. These problems can be mitigated, but not solved, by constrained LDA (cLDA) calculations,[8–10] which can be exploited to extract two independent parameters: interaction and double counting correction.[9,11]

A conceptually preferable and better defined many-body approach is achieved if one substitutes LDA by the so-called GW approximation.[12,13] Since its proposition by Biermann *et al.*,[14] the development and application of such a GW + DMFT scheme for actual applications has been tedious. This is reflected in the number of LDA + DMFT calculations for actual materials, which is of the order of a few hundred, compared to two GW + DMFT calculations, one for Ni (Ref. 14) and one for $SrVO_3$,[15] despite many advantages of GW + DMFT, such as the possible rigorous definition in terms of Feynman diagrams and the avoidance of introducing ad hoc parameters for the Coulomb interaction and double counting corrections. The reason for this imbalance is twofold. First, since the GW approach is computationally fairly demanding and complex, mature GW programs were missing in the past. Second, the GW + DMFT scheme is considerably more involved than LDA + DMFT, in particular, if calculations are done self-consistently and with a frequency dependent (screened) Coulomb interaction. Indeed, these concepts are presently tested on the model level.[16,17] Let us also note in this context that a frequency dependent interaction has been employed on top of an LDA band structure for $BaFe_2As_2$ (Ref. 18) and $SrVO_3$.[19]

In this paper we present results for a simplified quasiparticle (qp) GW + DMFT implementation in the Vienna *ab initio* simulation package (VASP) for $SrVO_3$ and compare the qpGW + DMFT results to those of LDA + DMFT[20] as well as photoemission spectroscopy.[21] We find the qpGW + DMFT spectra to be quite similar to that of LDA + DMFT due to a partial cancellation of two effects: The reduced GW bandwidth in comparison to LDA and the weaker screened Coulomb interaction. An important difference, however, is the position of the lower Hubbard band, which in qpGW + DMFT better agrees with experiment. To mimic the frequency dependence of the Coulomb interaction, which we have not included, we also performed qpGW + DMFT calculations including a $\mathcal{Z}_B$ factor reduced bandwidth as suggested by Casula *et al.*[23] The obtained spectra are rather different from qpGW + DMFT without $\mathcal{Z}_B$-reduced bandwidth and LDA + DMFT.

The paper is organized as follows: In Sec. II we discuss the method and implementation. In Sec. III we compare LDA + DMFT and qpGW + DMFT self-energies and spectral functions. A comparison to photoemission experiments is provided in Sec. IV and a conclusion in Sec. V. The Appendix discusses the treatment of the double counting in the qpGW + DMFT scheme.

II. METHOD

Let us briefly outline the relevant methodological aspects. The starting point of our calculation is the GW implementation within (VASP).[24] Specifically, we first performed Kohn Sham density functional theory calculations using the local density

approximation for $SrVO_3$ at the LDA lattice constant of $a = 3.78$ Å and determined the Kohn Sham one-electron orbitals $\phi_{n\mathbf{k}}$ and one-electron energies $\epsilon_{n\mathbf{k}}$. The position of the GW quasiparticle peaks were calculated by solving the linear equation

$$E^{\mathrm{qp}}_{n\mathbf{k}} = \epsilon_{n\mathbf{k}} + Z_{n\mathbf{k}}\mathrm{Re}[\langle\phi_{n\mathbf{k}}|T + V_{n\text{-}e} + V_H + \Sigma(\epsilon_{n\mathbf{k}})|\phi_{n\mathbf{k}}\rangle - \epsilon_{n\mathbf{k}}], \quad (1)$$

where T is the one-electron kinetic energy operator and $V_{n\text{-}e}$ and V_H are the nuclear-electron potential and the Hartree potential, respectively. Σ is the G_0W_0 self-energy, and $Z_{n\mathbf{k}}$ is the renormalization factor evaluated at the Kohn-Sham eigenvalues.[24,25] The original Kohn Sham orbitals are maintained at this step. The Kohn Sham orbitals expressed in the projector augmented wave (PAW) basis are then projected onto maximally localized Wannier functions[26] using the Wannier90 code.[27,28] To construct an effective low-energy Hamiltonian for the t_{2g} vanadium orbitals, we follow Faleev, van Schilfgaarde, and Kotani and approximate the frequency dependent G_0W_0 self-energy by an Hermitian operator $\bar{H}$ that reproduces the position of the quasiparticle peaks of the original self-energy exactly:[29,30]

$$\bar{H}_{mn,\mathbf{k}} = \tfrac{1}{2}\left[\langle\phi_{m\mathbf{k}}|\Sigma^*\left(E^{\mathrm{qp}}_{m\mathbf{k}}\right) + \Sigma\left(E^{\mathrm{qp}}_{n\mathbf{k}}\right)|\phi_{n\mathbf{k}}\rangle\right]. \quad (2)$$

This qp approximation is commonly used in GW calculations, in particular for self-consistent calculations, since fully frequency dependent calculations are computationally very demanding.

In practice, for the present calculations, we have applied the slightly more involved procedure to derive an Hermitian approximation outlined in Ref. 31, although this yields essentially an almost identical Hermitian operator $\bar{H}_{mn,\mathbf{k}}$. Furthermore, the of-diagonal components are found to be negligibly small, and henceforth disregarded. The final Hermitian and $\mathbf{k}$-point dependent operator $\bar{H}$ is transformed to the Wannier basis and passed on to the DMFT code, where it is used to construct the $\mathbf{k}$-dependent self-energy by adding the local DMFT self-energy.

This qpGW + DMFT procedure allows us to maintain the structure and outline of the common DFT-DMFT scheme and can be easily adopted in any DMFT code. Instead of the LDA one-electron matrix elements, the qpGW ones are passed to the DMFT. This procedure neglects lifetime broadening and any frequency dependence of the GW self-energy beyond its linear part. Subtracting the local part of this qpGW Hermitian operator (to avoid a double counting, see the Appendix) yields for the degenerate t_{2g} orbitals basically a constant shift. Let us also note that hitherto we did not perform self-consistency on the GW part.

Figure 1 shows the obtained G_0W_0 band structure, which for the t_{2g} vanadium target bands is about 0.7 eV narrower than for the LDA. The oxygen p band (below -2 eV) is shifted downwards by 0.5 eV compared to the LDA, whereas the vanadium e_g bands (located about 1.5 eV above the Fermi level) are slightly shifted upwards by 0.2 eV. In the LDA, the top most vanadium t_{2g} band at the M point is slightly above the lowest e_g band at the Γ point, whereas the G_0W_0 correction opens a gap between the t_{2g} and e_g states.

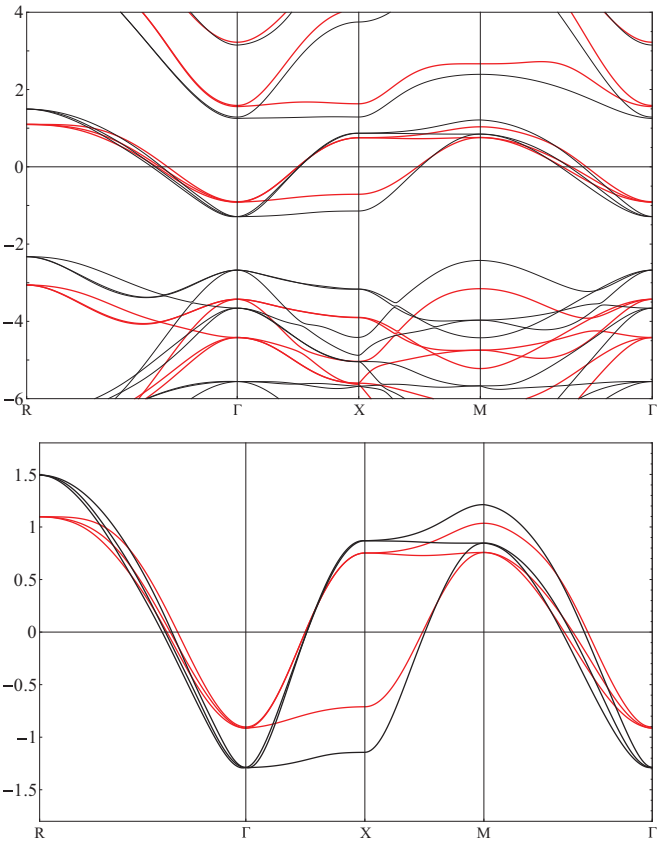

FIG. 1. (Color online) Upper panel: G_0W_0 quasiparticle bands (red, gray) in comparison to LDA (black). The Fermi level sets our zero of energy and is marked as a line. Lower panel: Wannier projected t_{2g} band structure from G_0W_0 (red, gray) and LDA (black). The t_{2g} target bands bandwidth is reduced by ∼0.7 eV in GW.

Within this Wannier basis, we also calculate the screened Coulomb interaction using the random phase approximation (RPA). As described in Ref. 32, for an accurate estimate of the interaction value to be used in DMFT (U^{DMFT}), only the local screening processes of the t_{2g} target bands of $SrVO_3$ are disregarded since only these are considered later on in DMFT. This approach[32] is similar to the constrained RPA (cRPA),[33,34] with the difference being that in cRPA also *nonlocal* screening processes of the t_{2g} target bands are disregarded, since these are not included in DMFT either. Depending on the material and doping level, there might be a difference between U^{DMFT} and U^{cRPA}. However, for the case of $SrVO_3$, this difference is very minor, and we hence only consider U^{DMFT} in the following. We carefully compare qpGW + DMFT with LDA + DMFT calculations and experiment. In both cases, we use (frequency-independent) interactions obtained from this locally unscreened RPA and cLDA. The Kanamori interaction parameters as derived from the locally unscreened RPA are intraorbital Coulomb repulsion $U^{\mathrm{DMFT}} = 3.44$ eV; interorbital Coulomb repulsion $\bar{U}^{\mathrm{DMFT}} = 2.49$ eV; and Hund's exchange and pair hopping amplitude $J^{\mathrm{DMFT}} = 0.46$ eV.[35] These values are, for $SrVO_3$, almost identical to the cRPA.[32] In cLDA, on the other hand, somewhat larger interaction parameters were obtained and are employed by us for the corresponding calculations $U^{\mathrm{cLDA}} = 5.05$ eV, $\bar{U}^{\mathrm{cLDA}} = 3.55$ eV, and $J^{\mathrm{cLDA}} = 0.75$ eV.[21,36]

For the subsequent DMFT calculation we employ the Würzburg-Wien *w2dynamics* code,[38] based on the hybridization-expansion variant[39] of the continuous-time quantum Monte Carlo method (CT-QMC).[40] This algorithm is particularly fast since it employs additional quantum numbers for a rotationally invariant Kanamori interaction.[38] The maximum entropy method is employed for the analytical continuation of the imaginary time and (Matsubara) frequency CT-QMC data to real frequencies.[41]

All our calculations are without self-consistency, which is to some extent justified for $SrVO_3$. Since the three t_{2g} bands of $SrVO_3$ are degenerate, DMFT does not change the charge density of the low-energy t_{2g} manifold and hence self-consistency effects are expected to be small for LDA + DMFT. This is, in principle, different for qpGW + DMFT. Here the frequency dependence of the DMFT self-energy might yield some feedback already for a simplified Faleev, van Schilfgaarde, and Kotani quasiparticle self-consistency.[29,30] Finally, we also test the $\mathcal{Z}_B$-factor renormalized GW bandwidth with $\mathcal{Z}_B = 0.7$ obtained in Ref. 23 for mimicking the frequency dependence of the cRPA interaction.

III. RESULTS

For analyzing the differences between qpGW + DMFT and LDA + DMFT we analyze and compare five different calculations in the following:

(1) LDA + DMFT@$\bar{U}^{\mathrm{cLDA}}$ (conventional LDA + DMFT calculation with the cLDA interaction $\bar{U}^{\mathrm{cLDA}} = 3.55$ eV).

(2) LDA + DMFT@$\bar{U}^{\mathrm{DMFT}}$ (LDA + DMFT calculation but with the locally unscreened RPA interaction $\bar{U}^{\mathrm{DMFT}} = 2.49$ eV).

(3) qpGW + DMFT@$\bar{U}^{\mathrm{DMFT}}$ (qpGW + DMFT calculation with $\bar{U}^{\mathrm{DMFT}} = 2.49$ eV).

(4) qpGW + DMFT@$\bar{U}^{\mathrm{cLDA}}$ (qpGW + DMFT calculation but with $\bar{U}^{\mathrm{cLDA}} = 3.55$ eV).

(5) qpGW + DMFT@$\bar{U}^{\mathrm{DMFT}}$,$\mathcal{Z}_B = 0.7$ (as 3 but with a Bose renormalization factor $\mathcal{Z}_B$).

Let us first turn to the imaginary part of the local self-energy which is shown as a function of (Matsubara) frequency in Fig. 2. The self-energy yields a first impression of how strong the electronic correlations are in the various calculations. The LDA + DMFT@$\bar{U}^{\mathrm{DMFT}}$ self-energy is the least correlated one, somewhat less correlated than LDA + DMFT@$\bar{U}^{\mathrm{cLDA}}$ due to the smaller locally unscreened Coulomb interaction ($\bar{U}^{\mathrm{DMFT}} = 2.49 < 3.55$ eV $= \bar{U}^{\mathrm{cLDA}}$). For the same reason also the qpGW + DMFT@$\bar{U}^{\mathrm{DMFT}}$ self-energy is less correlated than that of a qpGW + DMFT@$\bar{U}^{\mathrm{cLDA}}$ calculation.

If we compare LDA + DMFT and qpGW + DMFT on the other hand, the LDA + DMFT self-energy is less correlated than the qpGW + DMFT one, if the Coulomb interaction is kept the same. This is due to the 0.7 eV smaller GW t_{2g} bandwidth in comparison to LDA. This observation also reflects in the DMFT quasiparticle renormalization factors Z, which were obtained from a fourth-order fit to the lowest four Matsubara frequencies, see Table I. Also there is an additional GW renormalization factor reducing the bandwidth in comparison to LDA.

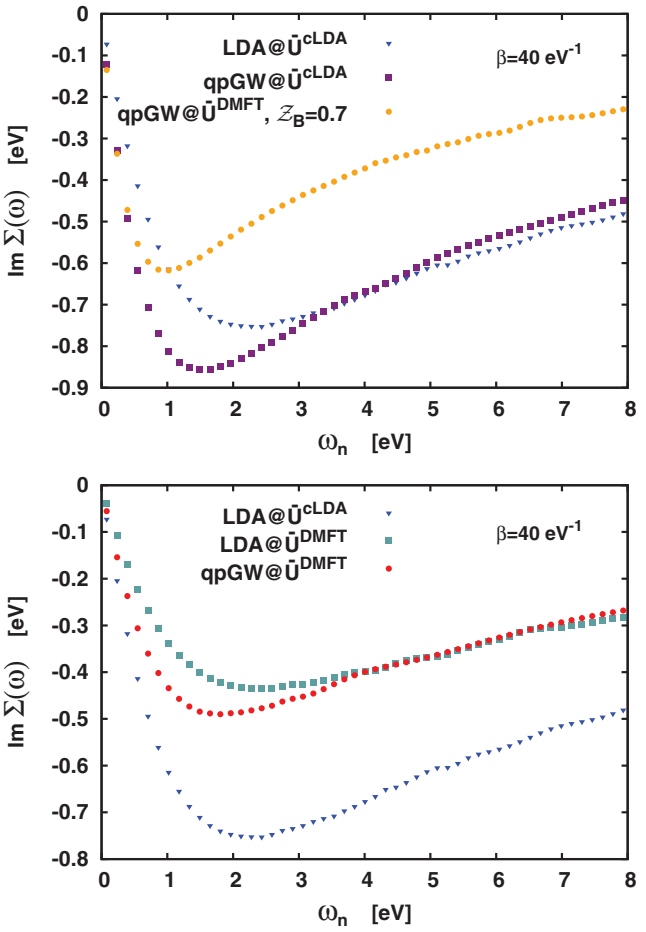

FIG. 2. (Color online) Comparison of the imaginary part of the DMFT t_{2g} self-energies Σ vs (Matsubara) frequency ω for $SrVO_3$ at inverse temperature $\beta = 40$ eV^{-1} as computed in five different ways: employing qpGW and LDA Wannier bands, the locally unscreened RPA interaction $\bar{U}^{\mathrm{DMFT}} = 2.49$ eV and the cLDA $\bar{U}^{\mathrm{cLDA}} = 3.55$ eV, as well as the $\mathcal{Z}_B = 0.7$ renormalization.[23]

TABLE I. DMFT quasiparticle renormalization factors Z from the five different calculations at inverse temperature $\beta = 40$ eV^{-1}. Also shown are the pairwise double occupations within the same orbital d_{intra} and between different orbitals with the same $d^{\uparrow\uparrow}_{\mathrm{inter}}$ and opposite spin $d^{\uparrow\downarrow}_{\mathrm{inter}}$. The "standard" LDA + DMFT@$\bar{U}^{\mathrm{cLDA}}$ and qpGW + DMFT@$\bar{U}^{\mathrm{DMFT}}$ calculations are similarly correlated and agree well with experiment. Using the cLDA interaction($\bar{U}^{\mathrm{cLDA}}$) for qpGW + DMFT or the locally unscreened RPA ($\bar{U}^{\mathrm{DMFT}}$) for LDA + DMFT yields a too strongly and too weakly correlated solution in comparison to experiment, respectively. Note that qpGW + DMFT becomes even more strongly correlated if the Bose renormalization factor is included.

Scheme	Z	d_{intra}	$d^{\uparrow\uparrow}_{\mathrm{inter}}$	$d^{\uparrow\downarrow}_{\mathrm{inter}}$
LDA + DMFT@$\bar{U}^{\mathrm{cLDA}}$	0.51	0.004	0.013	0.009
LDA + DMFT@$\bar{U}^{\mathrm{DMFT}}$	0.67	0.007	0.016	0.013
qpGW + DMFT@$\bar{U}^{\mathrm{DMFT}}$	0.57	0.005	0.014	0.010
qpGW + DMFT@$\bar{U}^{\mathrm{cLDA}}$	0.39	0.003	0.010	0.007
qpGW + DMFT@$\bar{U}^{\mathrm{DMFT}}$, $\mathcal{Z}_B = 0.7$	0.36	0.003	0.009	0.006
Experiment[21,43]	∼0.5–0.6			

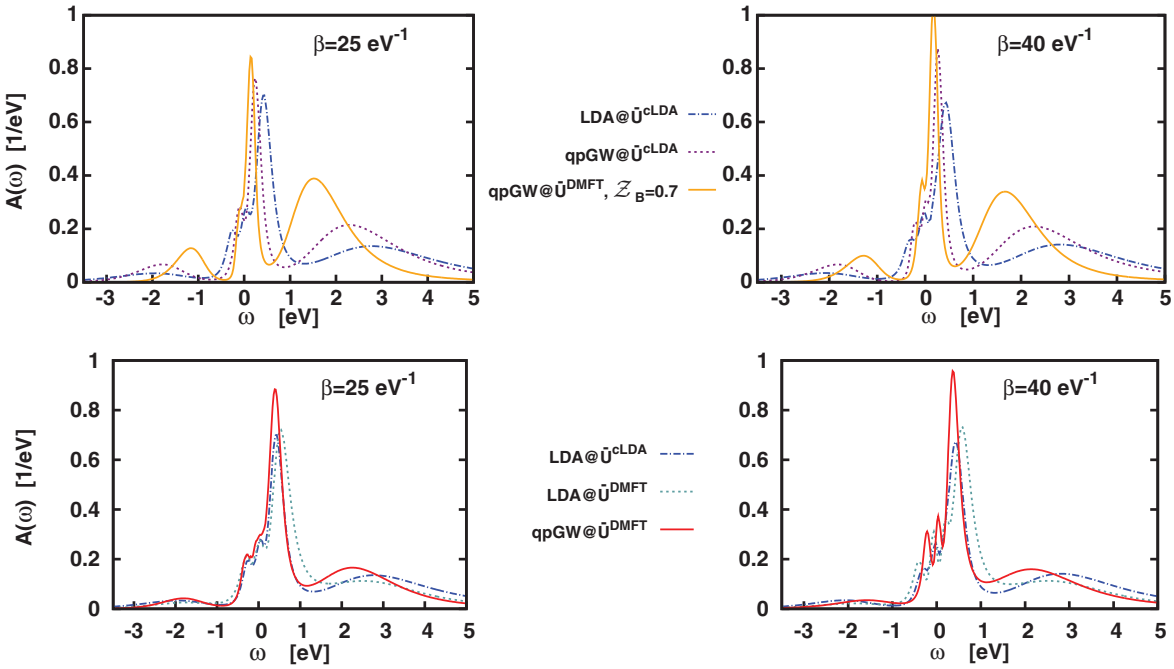

FIG. 3. (Color online) Spectral function for $SrVO_3$ (t_{2g} orbitals only) computed in five different ways as in Fig. 2. At lower temperatures the central peak gets only slightly sharper and higher, although the temperature effects from $\beta = 25$ to 40 eV^{-1} are small.

However, the effect of the smaller GW bandwidth partially compensates with the smaller $\bar{U}^{\mathrm{DMFT}}$ interaction strength. Altogether this yields rather similar self-energies of the standard approaches: LDA + DMFT@$\bar{U}^{\mathrm{cLDA}}$ and qpGW + DMFT@$\bar{U}^{\mathrm{DMFT}}$, see lower panel of Fig. 2. This also reflects in very similar renormalization factors in Table I, $Z = 0.51$ vs $Z = 0.57$, which both agree well with experimental estimates of 0.5–0.6.[21,42,43]

Since one important difference is the strength of the interaction, it is worthwhile recalling that $\bar{U}^{\mathrm{DMFT}}$ is defined as the local interaction strength at low frequencies. While this value is almost constant within the range of the t_{2g} bandwidth, it approaches the bare Coulomb interaction at larger energies, exceeding 10 eV. It has been recently argued and shown in model calculations[23] that the stronger frequency dependence of the screened Coulomb interaction at high energies is of relevance and can be mimicked by a $\mathcal{Z}_B$ renormalization of the GW bandwidth. The latter has been determined as $\mathcal{Z}_B = 0.7$ for $SrVO_3$. We have tried to take this into account in the qpGW + DMFT@$\bar{U}^{\mathrm{DMFT}}$, $\mathcal{Z}_B = 0.7$ calculation. Due to the additional bandwidth renormalization, this calculation is very different from all others and yields the largest quasiparticle renormalization, i.e., $Z = 0.36$ is smallest.

This too small quasiparticle weight can be understood as follows: The $\mathcal{Z}_B$ factor mimics the frequency dependence of cRPA screened Coulomb interaction, which is much larger at high frequencies. In a fully frequency dependent GW calculation, this is properly matched by a correspondingly large GW self-energy at large frequencies. However, within the quasiparticle treatment of the GW self-energy (which represents a linear approximation to its frequency dependence, see the Appendix) such high frequency contributions of the GW self-energy are not included. As our results show, in this case, it is hence more consistent not to include the frequency dependence for the Coulomb interaction only, which the $\mathcal{Z}_B$ factor emulates.

Next, we compare the **k**-integrated spectrum in Fig. 3. At low frequency we find the same trends as for the self-energy results: the qpGW + DMFT and LDA + DMFT at $\bar{U}^{\mathrm{DMFT}}$ and $\bar{U}^{\mathrm{cLDA}}$, respectively, yield a rather similar spectrum. In particular, the quasiparticle peak has a similar weight and shape. However, a difference is found at larger frequencies: The qpGW + DMFT Hubbard bands are closer to the Fermi level in comparison to LDA + DMFT (see Sec. IV). If we perform qpGW + DMFT and LDA + DMFT at the "wrong" interaction strength (i.e., $\bar{U}^{\mathrm{cLDA}}$ and $\bar{U}^{\mathrm{DMFT}}$, respectively), we obtain a noticeably stronger and weaker correlated solution, respectively. This trend is also reflected in the double occupations presented in Table I. Finally, as in the case of the self-energy, the qpGW + DMFT@$\bar{U}^{\mathrm{DMFT}}$, $\mathcal{Z}_B = 0.7$ solution is much more strongly correlated, with Hubbard side bands at much lower energies.

IV. COMPARISON TO PHOTOEMISSION SPECTROSCOPY

An obvious question is whether LDA + DMFT or qpGW + DMFT yields "better" results. This question is difficult to answer and for the time being we resort to a comparison with experimental photoemission spectroscopy (PES).[21] However, one should be well aware of the limitations of such a comparison. On the theory side, the involved approximations common to the calculations, as, e.g., neglecting nonlocal correlations beyond the DMFT and GW level, or further effects, such as the electron-phonon coupling or the photoemission matrix elements, might bias the theoretical result in one way or the other. On the experimental side, care is in place, as well, although the PES results have considerably improved in the last years due to better photon sources.

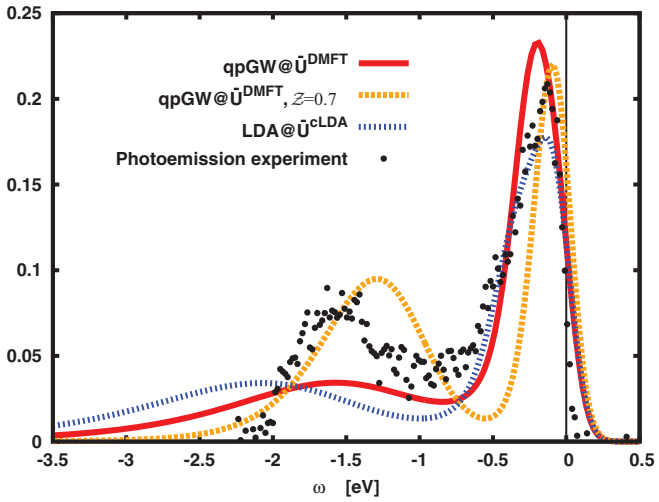

FIG. 4. (Color online) Comparison of LDA + DMFT@U^{cLDA}, qpGW + DMFT@U^{DMFT} (without and with Bose renormalization $\mathcal{Z}_B = 0.7$), and experiment. The position of the lower Hubbard band is better reproduced in qpGW + DMFT, whereas the central peak is similar in LDA + DMFT and qpGW + DMFT. The Bose renormalization qpGW + DMFT differs considerably (photoemission spectra reproduced from Ref. 21).

Furthermore, in Ref. 21 an oxygen p background has been subtracted, which by construction removes all spectral weight below the region identified as the lower Hubbard band.

Figure 4 compares the proposed LDA + DMFT and qpGW + DMFT (with and without Bose renormalization) with PES experiment. To this end, the theoretical results have been multiplied with the Fermi function at the experimental temperature of 20 K and broadened by the experimental resolution of 0.1 eV. The height of the PES spectrum has been fixed so that its integral yields 1, i.e., accommodates one t_{2g} electron, as in theory.

The qpGW + DMFT@$\bar{U}^{\mathrm{DMFT}}$ and LDA + DMFT@$\bar{U}^{\mathrm{cLDA}}$ have a quite similar quasiparticle peak, which also well agrees with experiment, as it was already indicated by the quasiparticle renormalization factor. A noteworthy difference is the position of the lower Hubbard band which is at -2 eV for LDA + DMFT@$\bar{U}^{\mathrm{cLDA}}$ and ~ -1.6 eV for qpGW + DMFT@$\bar{U}^{\mathrm{DMFT}}$. The latter is in agreement with experiment and a result of the reduced GW bandwidth. Let us note that the sharpness and height of the lower Hubbard band very much depends on the maximum entropy method, which tends to overestimate the broadening of the high-energy spectral features. Hence, only the position and weight is a reliable result of the calculation.

As we have already seen, the Bose-factor renormalized qpGW + DMFT@$\bar{U}^{\mathrm{DMFT}}$, $\mathcal{Z}_B = 0.7$ calculation is distinct from both qpGW + DMFT@$\bar{U}^{\mathrm{DMFT}}$ and LDA + DMFT@$\bar{U}^{\mathrm{cLDA}}$. It is also different from experiment with a much more narrow quasiparticle peak and a lower Hubbard band much closer to the Fermi level. A similar difference between static U on the one side and frequency dependent U was reported in Ref. 19. A difference of this magnitude is hence to be expected. Recently we became aware of Ref. 44, in which Tomczak *et al.* report a qpGW + DMFT calculation with the full frequency dependence of the cRPA interaction for $SrVO_3$ obtaining good agreement with experiment as well.

V. CONCLUSION

We have carried out a careful comparison of LDA + DMFT, qpGW + DMFT (specifically, quasiparticle G_0W_0 + DMFT), and experiment for the case of $SrVO_3$, which is often considered to be a "benchmark" material for new methods. To this end, the LDA or G_0W_0 quasiparticle band structure was projected onto maximally localized Wannier orbitals for the t_{2g} bands. For these in turn correlation effects have been calculated on the DMFT level. If we take the locally unscreened RPA interaction (or the similar cRPA one) for the qpGW + DMFT and the cLDA interaction for LDA + DMFT, the two approaches yield rather similar self-energies and spectral functions at the Fermi level. These also agree rather well with photoemission spectroscopy. A noteworthy difference between these two calculation is found, however, for the position of the lower Hubbard band, which is better reproduced in qpGW + DMFT. Similar spectra were also obtained by Tomczak *et al.*[44] using a GW + DMFT calculation including the frequency dependence of the interaction.

From a principle point of view also a LDA + DMFT calculation with a locally unscreened or cRPA Coulomb interaction is possible and employed in the literature. In the static limit, these cRPA interactions are typically smaller than cLDA values. At least for $SrVO_3$, these smaller interaction values yield too weak electronic correlations if used for LDA + DMFT calculations.

ACKNOWLEDGMENTS

We thank R. Arita, S. Biermann, K. Nakamura, Y. Nomura, M. Imada, S. Sakai, and J. Tomzcak for many helpful discussions. We acknowledge financial support from Austrian Science Fund (FWF), SFB ViCom F41 I597, and the DFG Research Unit FOR 1346. Calculations have been done on the Vienna Scientific Cluster (VSC).

APPENDIX

In this Appendix we briefly discuss the quasiparticle "Hermitization" that we employ to the G_0W_0 self-energy, and explain how to deal with the double counting within this approximation.

The quasiparticle eigenvalues are obtained by linearizing the G_0W_0 self-energy around the LDA single particle levels $\epsilon^0_{n\mathbf{k}}$:

$$\Sigma\left(\mathbf{k}, E^{\mathrm{qp}}_{n\mathbf{k}}\right) = \Sigma\left(\mathbf{k}, \omega = \epsilon^0_{n\mathbf{k}}\right) + \underbrace{\left.\frac{\partial \Sigma(\mathbf{k},\omega)}{\partial \omega}\right|_{\omega=\epsilon^0_{n\mathbf{k}}}}_{\equiv \xi_{n\mathbf{k}}} \left(E^{\mathrm{qp}}_{n\mathbf{k}} - \epsilon^0_{n\mathbf{k}}\right). \quad \text{(A1)}$$

Since the off-diagonal components are small, we concentrate here on the diagonal components only. This yields the following equation for the quasiparticle poles:

$$E^{\mathrm{qp}}_{n\mathbf{k}} \langle \phi_{n\mathbf{k}} | 1 - \xi_{n\mathbf{k}} | \phi_{n\mathbf{k}} \rangle = \langle \phi_{n\mathbf{k}} | T + V_{n\text{-}e} + V_H + \Sigma\left(\mathbf{k}, \epsilon^0_{n\mathbf{k}}\right) - \xi_{n\mathbf{k}} \epsilon^0_{n\mathbf{k}} | \phi_{n\mathbf{k}} \rangle, \quad \text{(A2)}$$

which is the same as Eq. (1), except for substituting the derivative of the self-energy by $Z_{n\mathbf{k}} = (1 - \xi_{n\mathbf{k}})^{-1}$. For these diagonal elements, Hermitization involves just setting the imaginary part to zero. Generalization of this equation to the nondiagonal components is given in Ref. 31.

Since in DMFT the local contribution of the exchange-correlation term is considered as well, we need to subtract this contribution to avoid a double counting. This can be done by subtracting the local part of all qpGW self-energy contributions, i.e., the local part of the $\Sigma(\mathbf{k},\epsilon^0_{n\mathbf{k}})$, $\xi_{n\mathbf{k}}$, and $\xi_{n\mathbf{k}}\epsilon^0_{n\mathbf{k}}$ terms in Eq. (A2). We define their local part as the one-center $\mathbf{R} = 0$ component of the Wannier representation:

$$\overline{A}_{ij} = \frac{1}{N_k}\sum_{n\mathbf{k}} U^{*(\mathbf{k})}_{in} A_n(\mathbf{k}) U^{(\mathbf{k})}_{jn}. \tag{A3}$$

where N_k is the number of k points and $U^{(\mathbf{k})}_{in}$ is the unitary matrix for the transformation of Bloch vectors $|\phi_{n\mathbf{k}}\rangle$ to Wannier states $|w_{i\mathbf{0}}\rangle$. For $A_n(\mathbf{k}) = \Sigma(\mathbf{k},\epsilon^0_{n\mathbf{k}})$, $\xi_{n\mathbf{k}}$, and $\xi_{n\mathbf{k}}\epsilon^0_{n\mathbf{k}}$ these averages are computed, transformed back to the Bloch basis using again $U^{(\mathbf{k})}_{ni}$, and subtracted in Eq. (A2). With the local part subtracted, Eq. (A2) becomes

$$\begin{aligned} E^{\mathrm{qp-nl}}_{n\mathbf{k}} &\langle\phi_{n\mathbf{k}}|1 - \xi_{n\mathbf{k}} + \overline{\xi}_n|\phi_{n\mathbf{k}}\rangle \\ &= \langle\phi_{n\mathbf{k}}|T + V_{n\text{-}e} + V_H + \Sigma\left(\mathbf{k},\epsilon^0_{n\mathbf{k}}\right) \\ &\quad - \overline{\Sigma}_n - \xi_{n\mathbf{k}}\epsilon^0_{n\mathbf{k}} + \overline{\xi\epsilon^0_n}|\phi_{n\mathbf{k}}\rangle. \end{aligned} \tag{A4}$$

This yields the band structure without local quasiparticle self-energy contributions. The Hamiltonian corresponding to this band structure is subsequently transformed again to the Wannier basis and passed to the DMFT.

Let us emphasize that this local part of the *quasiparticle* GW self-energy is very different from the local part of a frequency-dependent full GW self-energy. In the latter case we naturally also obtain a frequency-dependent local part $\Sigma^{GW}_{\mathrm{loc.}} = \sum_k \Sigma(\mathbf{k},\omega)$. In our case of the quasiparticle linearization of the GW self-energy [Eq. (A1)], we obtain three frequency-independent terms stemming from the constant [$\overline{\Sigma}_n$] and linear terms [$\overline{\xi}_n$ and $\overline{\xi\epsilon^0_n}$] in Eq. (A1), respectively. This is consistent with the qpGW approximation. Let us note though that doing (i) the qp approximation and (ii) subtracting the local part does not commute.

[1] V. I. Anisimov, A. I. Poteryaev, M. A. Korotin, A. O. Anokhin, and G. Kotliar, J. Phys.: Condens. Matter **9**, 7359 (1997).

[2] A. I. Lichtenstein and M. I. Katsnelson, Phys. Rev. B **57**, 6884 (1998).

[3] K. Held, I. A. Nekrasov, G. Keller, V. Eyert, N. Blümer, A. K. McMahan, R. T. Scalettar, T. Pruschke, V. I. Anisimov, and D. Vollhardt, Psi-k Newsletter **56**, 5 (2003); Phys. Status Solidi B **243**, 2599 (2006).

[4] G. Kotliar, S. Y. Savrasov, K. Haule, V. S. Oudovenko, O. Parcollet, and C. A. Marianetti, Rev. Mod. Phys. **78**, 865 (2006).

[5] K. Held, Adv. Phys. **56**, 829 (2007).

[6] W. Metzner and D. Vollhardt, Phys. Rev. Lett. **62**, 324 (1989); A. Georges and G. Kotliar, Phys. Rev. B **45**, 6479 (1992).

[7] A. Georges, G. Kotliar, W. Krauth, and M. Rozenberg, Rev. Mod. Phys. **68**, 13 (1996).

[8] P. H. Dederichs, S. Blügel, R. Zeller, and H. Akai, Phys. Rev. Lett. **53**, 2512 (1984).

[9] A. K. McMahan, R. M. Martin, and S. Satpathy, Phys. Rev. B **38**, 6650 (1988).

[10] O. Gunnarsson, O. K. Andersen, O. Jepsen, and J. Zaanen, Phys. Rev. B **39**, 1708 (1989).

[11] For an example where U and the double counting correction have actually been obtained independently see A. K. McMahan, C. Huscroft, R. T. Scalettar, and E. L. Pollock, J. Comput.-Aided Mol. Design **5**, 131 (1998).

[12] L. Hedin, Phys. Rev. A **139**, 796 (1965).

[13] F. Aryasetiawan and O. Gunnarsson, Rep. Prog. Phys. **61**, 237 (1998).

[14] S. Biermann, F. Aryasetiawan, and A. Georges, Phys. Rev. Lett. **90**, 086402 (2003).

[15] Recently we became aware of a second GW + DMFT calculation: in a most recent preprint[44] Tomczak *et al.* studied, independently of us, $SrVO_3$ as well.

[16] P. Sun and G. Kotliar, Phys. Rev. B **66**, 085120 (2002).

[17] T. Ayral, P. Werner, and S. Biermann, Phys. Rev. Lett. **109**, 226401 (2012); T. Ayral, S. Biermann, and P. Werner, Phys. Rev. B **87**, 125149 (2013).

[18] P. Werner, M. Casula, T. Miyake, F. Aryasetiawan, A. J. Millis, and S. Biermann, Nat. Phys. **8**, 331 (2012).

[19] M. Casula, A. Rubtsov, and S. Biermann, Phys. Rev. B **85**, 035115 (2012).

[20] Let us note that $SrVO_3$ is the material arguably most well investigated by LDA + DMFT. Previous LDA + DMFT calculations include Refs. 21, 22, and 45–47, cf. Ref. 19.

[21] A. Sekiyama, H. Fujiwara, S. Imada, S. Suga, H. Eisaki, S. I. Uchida, K. Takegahara, H. Harima, Y. Saitoh, I. A. Nekrasov, G. Keller, D. E. Kondakov, A. V. Kozhevnikov, Th. Pruschke, K. Held, D. Vollhardt, and V. I. Anisimov, Phys. Rev. Lett. **93**, 156402 (2004).

[22] I. A. Nekrasov, G. Keller, D. E. Kondakov, A. V. Kozhevnikov, T. Pruschke, K. Held, D. Vollhardt, and V. I. Anisimov, Phys. Rev. B **72**, 155106 (2005).

[23] M. Casula, P. Werner, L. Vaugier, F. Aryasetiawan, T. Miyake, A. J. Millis, and S. Biermann, Phys. Rev. Lett. **109**, 126408 (2012).

[24] M. Shishkin and G. Kresse, Phys. Rev. B **74**, 035101 (2006).

[25] M. S. Hybertsen and S. G. Louie, Phys. Rev. B **34**, 5390 (1986).

[26] N. Marzari and D. Vanderbilt, Phys. Rev. B **56**, 12847 (1997).

[27] C. Franchini, R. Kovacik, M. Marsman, S. Sathyanarayana Murthy, J. He, C. Ederer, and G. Kresse, J. Phys.: Condens. Matter **24**, 235602 (2012).

[28] A. A. Mostofi, J. R. Yates, Y.-S. Lee, I. Souza, D. Vanderbilt, and N. Marzari, Comput. Phys. Commun. **178**, 685 (2008).

[29] S. V. Faleev, M. van Schilfgaarde, and T. Kotani, Phys. Rev. Lett. **93**, 126406 (2004).

[30] A. N. Chantis, M. van Schilfgaarde, and T. Kotani, Phys. Rev. Lett. **96**, 086405 (2006).

[31] M. Shishkin, M. Marsman, and G. Kresse, Phys. Rev. Lett. **99**, 246403 (2007).

[32] Y. Nomura, M. Kaltak, K. Nakamura, C. Taranto, S. Sakai, A. Toschi, R. Arita, K. Held, G. Kresse, and M. Imada, Phys. Rev. B **86**, 085117 (2012).

[33] F. Aryasetiawan, M. Imada, A. Georges, G. Kotliar, S. Biermann, and A. I. Lichtenstein, Phys. Rev. B **70**, 195104 (2004).

[34] T. Miyake, F. Aryasetiawan, and M. Imada, Phys. Rev. B **80**, 155134 (2009).

[35] Note that the values differ slightly from the VASP values published in Ref. 32 since with additional data we have further improved the extrapolation.

[36] Note that cLDA tends to overestimate the Hund's exchange J, see Ref. 5, so that in subsequent LDA + DMFT calculations smaller values of J have been employed.[37] For the d^1 system $SrVO_3$ this smaller value of J mainly influences the upper Hubbard band.

[37] P. Wissgott, J. Kuneš, A. Toschi, and K. Held, Phys. Rev. B **85**, 205133 (2012).

[38] N. Parragh, A. Toschi, K. Held, and G. Sangiovanni, Phys. Rev. B **86**, 155158 (2012).

[39] P. Werner, A. Comanac, L. de Medici, M. Troyer and A. J. Millis, Phys. Rev. Lett. **97**, 076405 (2006).

[40] A. N. Rubtsov and A. I. Lichtenstein, JETP Lett. **80**, 61 (2004).

[41] M. Jarrell and J. E. Gubernatis, Phys. Rep. **269**, 133 (1996).

[42] K. Maiti, U. Manju, S. Ray, P. Mahadevan, I. H. Inoue, C. Carbone, and D. D. Sarma, Phys. Rev. B **73**, 052508 (2006); M. Takizawa, M. Minohara, H. Kumigashira, D. Toyota, M. Oshima, H. Wadati, T. Yoshida, A. Fujimori, M. Lippmaa, M. Kawasaki, H. Koinuma, G. Sordi, and M. Rozenberg, *ibid*. **80**, 235104 (2009)

[43] Note that due to the presence of kinks there are actually two such renormalization factors:[22,48,49] A Fermi liquid Z_{FL} for the renormalization at the lowest energies and a second Z_{CP} for higher energies. The latter also corresponds to the overall weight of the central peak. With the energy resolution in Fig. 2 being limited by the discrete Matsubara frequencies the Z of Table I still rather corresponds to Z_{CP} as do the experimental values of Refs. 21 and 42.

[44] J. M. Tomczak, M. Casula, T. Miyake, F. Aryasetiawan, and S. Biermann, Europhys. Lett. **100**, 67001 (2012).

[45] E. Pavarini, S. Biermann, A. Poteryaev, A. I. Lichtenstein, A. Georges, and O. K. Andersen, Phys. Rev. Lett. **92**, 176403 (2004).

[46] A. Liebsch, Phys. Rev. Lett. **90**, 096401 (2003).

[47] I. A. Nekrasov, K. Held, G. Keller, D. E. Kondakov, T. Pruschke, M. Kollar, O. K. Andersen, V. I. Anisimov, and D. Vollhardt, Phys. Rev. B **73**, 155112 (2006).

[48] K. Byczuk, M. Kollar, K. Held, Y.-F. Yang, I. A. Nekrasov, T. Pruschke, and D. Vollhardt, Nat. Phys. **3**, 168 (2007).

[49] S. Aizaki, T. Yoshida, K. Yoshimatsu, M. Takizawa, M. Minohara, S. Ideta, A. Fujimori, K. Gupta, P. Mahadevan, K. Horiba, H. Kumigashira, and M. Oshima, Phys. Rev. Lett. **109**, 056401 (2012).